10-1-2020

γ-Unstable Bohr Hamiltonian with sextic potential for odd-A nuclei

Hadi Sobhani
Shahrood University of Technology

Hassan Hassanabadi
Shahrood University of Technology

Dennis Bonatsos
Demokritos National Centre for Scientific Research

Feng Pan
Liaoning Normal University

Jerry P. Draayer
Louisiana State University

Recommended Citation

Sobhani, H., Hassanabadi, H., Bonatsos, D., Pan, F., & Draayer, J. (2020). γ-Unstable Bohr Hamiltonian with sextic potential for odd-A nuclei. *Nuclear Physics A, 1002* https://doi.org/10.1016/j.nuclphysa.2020.121956

γ-unstable Bohr Hamiltonian with sextic potential for odd-A nuclei

Hadi Sobhani[*1], *Hassan Hassanabadi*[1], *Dennis Bonatsos*[2], *Feng Pan*[3,4], and *Jerry P. Draayer*[4]

[1] *Faculty of Physics, Shahrood University of Technology, Shahrood, Iran*

[2] *Institute of Nuclear and Particle Physics, NCSR Demokritos, GR-15310 Aghia Paraskevi, Attiki, Greece*

[3] *Department of Physics, Liaoning Normal University, Dalian 116029, P. R. China*

[4] *Department of Physics and Astronomy, Louisiana State University, Baton Rouge, LA 70803-4001, USA*

June 1, 2020

Abstract

In this paper, odd-A nuclei in the vibrational to γ-soft transitional region are studied in the collective model, in which the odd-A system is described by the Bohr Hamiltonian with the quasi exactly solvable sextic β-part potential for the even-even core coupled with a single nucleon in a $j = 3/2$ orbit via the β-independent five-dimensional spin-orbit interaction and the total angular momentum degeneracy breaking term. To test the validity of the coupling scheme, we use the model to reproduce experimentally available level energies and B(E2) values of ^{187,189,191,193,195}Ir. It is clearly shown from both the level energies and the known B(E2) values for ^{191,193}Ir fitted that the model with the β-independent five-dimensional spin-orbit interaction and the total angular momentum degeneracy breaking term seems adequate to describe the low-lying level pattern and the structure of these odd-A nuclei.

[*] Electronic address: hadisobhani8637@gmail.com (Corresponding author)

1 Introduction

The critical point symmetries [1, 2] have been essential in understanding critical behaviors of shape (phase) transitions in nuclear structure [3–7] with the aim of analytical (exact or approximate) solutions [8,9] of the Bohr Hamiltonian in the collective model [10,11]. The critical point symmetry emerging at the critical point of the first order vibrational to the axially deformed rotational shape (phase) transition is the X(5) [2], while that emerging at the critical point of the second order vibrational to the γ-unstable phase transition is the E(5) [1, 12, 13]. These critical point symmetries can also be used to describe odd-A systems. For the first time Iachello suggested such an extension of the E(5) critical point symmetry [14,15]. It is shown that the E$(5/4)$ model may be used to describe an even-even system with the critical point E(5) symmetry coupled with a single nucleon in a $j = 3/2$ orbit. Further extension of the Bose-Fermi symmetry to the E(5/12) was made by Alonso, Arias, and Vitturi [16, 17] to include multi single-particle orbits, which provides a systematic way to describe the criticality in odd-A nuclei with a nucleon in $j = 1/2, 3/2, 5/2$ orbits. Similar extension of the X(5) model to odd-A case were also made. For example, Zhang et al followed the same manner of [14] and established $X(5/(2j+1))$ [18] and $X(3/(2j + 1))$ [19] models, for which further studies have been collected in [20–22].

In this paper, we intend to consider an even-even system confined in a sextic potential coupled with a single nucleon in a $j = 3/2$ orbit to describe odd-A nuclei in the vibrational to γ-soft transitional region. In fact, the γ-unstable Bohr Hamiltonian with a sextic potential for an even-even system is quasi-exactly solvable [23], which was studied by Lévai and Arias [24] for the first time and then applied to realistic nuclear systems by many others [25–31]. In what follows, theoretical basis of the γ-unstable Borh Hamiltonian for odd-A system is provided in Sec. 2. The sextic potential is introduced in Sec. 3, in which the solution of the eigenvalue problem is also provided. Numerical results and discussions are presented in the Sec. 4.

2 γ-unstable Bohr Hamiltonian for odd-A nuclei

In the collective model, an odd-A nucleus may be supposed as a single nucleon coupled to an even-even core. Therefore, the Hamiltonian of such a system is written in terms of that of the core part, the single particle (fermion part), and interactions of the core with the particle [15]

$$\hat{H} = \hat{H}_{\text{C}} + \hat{H}_{\text{F}} + kg(\beta)V_{\text{CF}} + k'g(\beta)\hat{J}\cdot\hat{J}, \tag{2.1}$$

where k and k' are free parameters. The core part of (2.1) is written in terms of the collective coordinates (β, γ) of the Bohr Hamiltonian

$$\hat{H}_{\text{C}} = -\frac{\hbar^2}{2B}\left[\frac{1}{\beta^4}\frac{\partial}{\partial\beta}\beta^4\frac{\partial}{\partial\beta} + \frac{1}{\beta^2\sin(3\gamma)}\frac{\partial}{\partial\gamma}\sin(3\gamma)\frac{\partial}{\partial\gamma} - \frac{1}{4\beta^2}\sum_{\kappa=1}^{3}\frac{\hat{Q}_\kappa^2}{\sin^2\left(\gamma - \frac{2\pi\kappa}{3}\right)}\right] + V(\beta,\gamma), \tag{2.2}$$

where the components of the angular momentum operator in the body-fixed coordinate system are denoted by $\hat{Q}_\kappa$. In the E(5/4) model the potential $V(\beta, \gamma)$ is considered only as a function of β leading to the γ-unstable structure. Thus, H_{C} can be separated into radial and angular parts with the wavefunction assumed to be a separable form $\Psi = F(\beta)\Phi(\gamma, \theta_i, \eta)$, in which η stands for the single-particle degrees of freedom. In this case, the γ-part of the wavefunction can be solved exactly as given by Bés [32]

$$\left[-\frac{1}{\sin(3\gamma)}\frac{\partial}{\partial\gamma}\sin(3\gamma)\frac{\partial}{\partial\gamma}+\frac{1}{4}\sum_{\kappa=1}^{3}\frac{\hat{Q}_{\kappa}^{2}}{\sin^{2}\left(\gamma-\frac{2\pi\kappa}{3}\right)}\right]\phi(\gamma,\theta_i)=\Lambda\phi(\gamma,\theta_i) \tag{2.3}$$

with eigenvalue $\Lambda=\tau(\tau+3)$, where τ is the seniority quantum number with $\tau=0,1,2,\cdots$. The final form of $\Phi(\gamma,\theta_i,\eta)$ is given by

$$\Phi(\gamma,\theta_i,\eta)=\sum_{L,M_L,m_j}\left\langle\begin{array}{cc|c}(\tau,0) & \left(\frac{1}{2},\frac{1}{2}\right) & \left(\tau,\frac{1}{2}\right)\\ L & 3/2 & J\end{array}\right\rangle\langle L\,M_L\;3/2\,m_j|J\,M_J\rangle\,\phi(\gamma,\theta_i)\chi_{3/2,m_j}(\eta), \tag{2.4}$$

where the first two symbols within the summation represent the isoscalar factor of Spin(5)⊃O(3) and the CG coefficient of O(3), respectively, and the single-particle wavefunction is denoted by $\chi_{j_F}(\eta)$ with $j_F=3/2$. The single-particle part $\hat{H}_F$ in (2.1) is a constant in this case, which is thus neglected. $V_{\rm CF}$ in (2.1) represents the interaction between the even-even core and the single-particle and is given by a five-dimensional spin-orbit interaction $\hat{\Lambda}\circ\hat{\Sigma}$. Finally, the total angular momentum degeneracy breaking term proportional to $J(J+1)$ is also added. Thus, the β-part eigen-equation is given by

$$\varphi''(\beta)+\left[\varepsilon-\frac{\Lambda}{\beta^2}-\frac{2B}{\hbar^2}g(\beta)\left(2k\left\langle\hat{\Lambda}\circ\hat{\Sigma}\right\rangle+k'\left\langle\hat{J}\cdot\hat{J}\right\rangle\right)-v(\beta)\right]\varphi(\beta)=0, \tag{2.5}$$

where $\varphi(\beta)=\beta^2F(\beta)$, $\varepsilon=\frac{2B}{\hbar^2}E$ is the reduced energy, $v(\beta)=\frac{2B}{\hbar^2}V(\beta)$ is the reduced potential,

$$\left\langle\hat{\Lambda}\circ\hat{\Sigma}\right\rangle=\frac{1}{2}\left[\tau_1\left(\tau_1+3\right)-\tau(\tau+3)-7/4\right],\quad\left\langle\hat{J}\cdot\hat{J}\right\rangle=J(J+1), \tag{2.6}$$

in which $\tau_1=\tau\pm1/2$, and $g(\beta)$ is considered to be the constant form with $g(\beta)=\hbar^2/2B$. Thus, (2.5) can be simplified as

$$\varphi''(\beta)+\left[\varepsilon'-\frac{\Lambda+2}{\beta^2}-v(\beta)\right]\varphi(\beta)=0, \tag{2.7}$$

$$\varepsilon'=\varepsilon-2k\left\langle\hat{\Lambda}\circ\hat{\Sigma}\right\rangle-k'J(J+1). \tag{2.8}$$

3 The sextic potential

In this section, the reduced potential $v(\beta)$ is considered to be a sextic polynomial form, of which a related one-dimensional Hamiltonian with the sextic potential and a centrifugal barrier can be written as [23, 24]

$$H=-\frac{d^2}{dx^2}+\frac{(2s-1/2)\,(2s-3/2)}{x^2}+c_{M,s}\,x^2+2ab\,x^4+a^2x^6, \tag{3.1}$$

where a, b, and s are real parameters, $x \in [0, \infty)$,

$$c_{M,s} = b^2 - 4a\left(s + \frac{1}{2} + M\right), \tag{3.2}$$

and M is a non-negative integer. This special potential is quasi-exactly solvable, which means that, for any non-negative integer value of M, its $M + 1$ solutions can be constructed algebraically. By substituting $x = \beta$ and $s = \tau/2 + 5/4$ in Eq. (3.1), it can be cast into Eq. (2.7). As shown in [24], in order to keep the potential $v(\beta)$ unchanged with τ, the non-negative integer M can be parameterized by the τ-dependent form with

$$M = M_0 - t \tag{3.3}$$

for both $\tau = 2t$ and $\tau = 2t + 1$ with $M_0 \geq t_{\max}$ and $t = 0, 1, 2, \cdots, t_{\max}$. Then, a constant v_0 should be added to the potential $v(\beta)$ for odd τ case such that the minimal of the original potential $v(\beta)$ for even τ and that of $v_0 + v(\beta)$ for odd τ are the same. In this work, because only $\tau \leq 3$ cases are considered, $M_0 = t_{\max} = 1$ is taken in the following. Our numerical results show that the constant v_0 for odd τ case is very small for $M_0 = 1$ considered, which is taken to be zero for simplicity.

The solution of the Hamiltonian (3.1) can be expressed as [23]

$$\varphi_n(x) = P_n\left(x^2\right)\left(x^2\right)^{s-1/4} \exp\left(-\frac{a}{4}x^4 - \frac{b}{2}x^2\right), \quad n = 0, 1, 2, \ldots, M, \tag{3.4}$$

where P_n is a polynomial of degree n, which is normalizable for $a \geq 0$ and reduces to the exactly solvable harmonic oscillator for $a = 0$. The $M = 0$ case corresponding to $\tau = 2$ and $\tau = 3$ contains only the nodeless solution. In this case, the eigen-energy is given by

$$E_0^{(M=0)} = 4bs \tag{3.5}$$

with the corresponding wave function

$$\varphi_0^{(M=0)}(x) \propto \left(x^2\right)^{s-1/4} \exp\left(-\frac{a}{4}x^4 - \frac{b}{2}x^2\right). \tag{3.6}$$

There are two solutions for $M = 1$ case corresponding to $\tau = 0$ and $\tau = 1$. The eigen-energies are given by

$$E_n^{(M=1)} = 4bs + \lambda_\pm(s), \tag{3.7}$$

in which

$$\lambda_\pm(s) = \begin{cases} 2b - 2\sqrt{b^2 + 8as}, & n = 0, \\ 2b + 2\sqrt{b^2 + 8as}, & n = 1. \end{cases} \tag{3.8}$$

The corresponding wave functions of this case are

$$\varphi_n^{(M=1)}(x) \propto \left(1 - \frac{\lambda_\pm}{8s}x^2\right)\left(x^2\right)^{s-1/4} \exp\left(-\frac{a}{4}x^4 - \frac{b}{2}x^2\right). \tag{3.9}$$

4 Results and applications to ^{187,189,191,193,195}Ir

In this section, we provide the model results of the related energy ratios and B(E2) values, which are then fitted to the corresponding experimental data of ^{187,189,191,193,195}Ir. The energy ratio is defined as

$$R_i = \frac{\varepsilon(n, \tau_1, J) - \varepsilon(0, 1/2, 3/2)}{\varepsilon(0, 3/2, 7/2) - \varepsilon(0, 1/2, 3/2)} \tag{4.1}$$

with $i \equiv \{n, \tau_1, J\}$, where n is the number of the nodes, τ is the seniority quantum number, $\tau_1 = \tau \pm 1/2$, and J is the total angular momentum. The allowed J values for a given τ_1 are listed in Table 1.

Table 1: The allowed angular momentum quantum number J for $\tau_1 \leq 7/2$.

τ_1	J							
$1/2$	$3/2$							
$3/2$	$7/2$	$5/2$	$1/2$					
$5/2$	$11/2$	$9/2$	$7/2$	$5/2$	$3/2$			
$7/2$	$15/2$	$13/2$	$11/2$	$9/2$	$9/2$	$7/2$	$5/2$	$3/2$

In fitting the experimental data, the fitting quality is measured by the χ^2 defined by

$$\chi^2 = \frac{\sum_{i=1}^{N} \left(R_i^{\text{Theo.}} - R_i^{\text{Exp.}} \right)^2}{N - N^*}, \tag{4.2}$$

where N is the numbers of the experimental data fitted, N^* is the number of the model parameters, $R_i^{\text{Theo.}}$ are the corresponding theoretical ratios, and $R_i^{\text{Exp.}}$ are the corresponding experimental ratios.

For the odd-A systems, the electromagnetic multipole transition operator involving the collective core and the (fermionic) single valence nucleon is defined as

$$T_{\mu}^{(\lambda)} = T_{C,\mu}^{(\lambda)} + T_{F,\mu}^{(\lambda)}, \tag{4.3}$$

where [15]

$$T_{C,\mu}^{(2)} = t_{21}\alpha_\mu + t_{22} \left(\alpha \times \alpha\right)_\mu^{(2)} \tag{4.4}$$

for $\lambda = 2$, in which t_{21} and t_{22} are parameters related to the effective charge of the core part, while the quadrupole deformation coordinates α_μ ($\mu = 0, \pm1, \pm2$) are related to the Bohr variables with

$$\alpha_\mu = \beta \left[D_{\mu\,0}^{(2)}(\theta_i) \cos\gamma + \left(D_{\mu\,2}^{(2)}(\theta_i) + D_{\mu\,-2}^{(2)}(\theta_i) \right) \sin\gamma \right], \tag{4.5}$$

and

$$T_{F,\mu}^{(2)} = t'_{22} \left(a_j^\dagger \times \widetilde{a}_j \right)_\mu^{(2)} \tag{4.6}$$

with the effective charge parameter of the valence nucleon t'_{22}, in which $a^{\dagger}_{j\mu}$ and $\tilde{a}_{j\mu} = (-)^{j-\mu} a_{j\,-\mu}$ are the valence nucleon creation and annihilation operators in the single-j shell, respectively. It is obvious that $T^{(2)}_C$ acts only on the core part and $T^{(2)}_F$ acts only on the single valence nucleon part of the wavefunction. For E2 transitions, the O(3)-reduced matrix element of the core part is given by

$$\begin{aligned}&\left\langle n'\tau'\tau'_1 J' \left|\left| T^{(2)}_C \right|\right| n\tau\tau_1 J \right\rangle \\ &= \sum_{L',L} \left\langle \begin{array}{cc|c} (\tau',0) & (\frac{1}{2},\frac{1}{2}) & (\tau'_1,\frac{1}{2}) \\ L' & \frac{3}{2} & J' \end{array} \right\rangle \left\langle \begin{array}{cc|c} (\tau,0) & (\frac{1}{2},\frac{1}{2}) & (\tau_1,\frac{1}{2}) \\ L & \frac{3}{2} & J \end{array} \right\rangle \\ &\times (-1)^{L+J+3/2} \left(2J'+1\right)^{1/2} \left(2J+1\right)^{1/2} \begin{Bmatrix} L' & J' & \frac{3}{2} \\ J & L & 2 \end{Bmatrix} \left\langle n'\tau' L' \left|\left| T^{(2)}_C \right|\right| n\tau L \right\rangle,\end{aligned} \tag{4.7}$$

where $\left\langle n'\tau' L' \left|\left| T^{(2)}_C \right|\right| n\tau L \right\rangle$ is related to the parameters t_{21} and t_{22} and provided in [33]. While the O(3)-reduced matrix element of $T^{(2)}_F$ is given by

$$\begin{aligned}&\left\langle n'\tau'\tau'_1 J' \left|\left| T^{(2)}_F \right|\right| n\tau\tau_1 J \right\rangle \\ &= \sum_{L} \left\langle \begin{array}{cc|c} (\tau,0) & (\frac{1}{2},\frac{1}{2}) & (\tau'_1,\frac{1}{2}) \\ L & \frac{3}{2} & J' \end{array} \right\rangle \left\langle \begin{array}{cc|c} (\tau,0) & (\frac{1}{2},\frac{1}{2}) & (\tau_1,\frac{1}{2}) \\ L & \frac{3}{2} & J \end{array} \right\rangle \\ &\times (-1)^{L+J+3/2} \left(2J'+1\right)^{1/2} \left(2J+1\right)^{1/2} \begin{Bmatrix} \frac{3}{2} & J' & L \\ J & \frac{3}{2} & 2 \end{Bmatrix} \delta_{n',n}\delta_{\tau',\tau} \left\langle \frac{3}{2} \left|\left| T^{(2)}_F \right|\right| \frac{3}{2} \right\rangle,\end{aligned} \tag{4.8}$$

where $\left\langle \frac{3}{2} \left|\left| T^{(2)}_F \right|\right| \frac{3}{2} \right\rangle = -\sqrt{5}\, t'_{22}$.

Thus, B(E2) value for the transition $n\tau L\, J \rightarrow n'\tau' L'\, J'$ is given by

$$\mathrm{B}\left(\mathrm{E2}; n\tau L J \rightarrow n'\tau' L' J'\right) = \frac{1}{2J+1} \left| \left\langle n'\tau' L' J' \left|\left| \left(T^{(2)}_C + T^{(2)}_F\right) \right|\right| n\tau L J \right\rangle \right|^2. \tag{4.9}$$

The selection rule of the $T^{(2)}_F$ is $\Delta\tau = \tau - \tau' = 0$. In our calculation, the second order term involved in the core part shown in (4.4) is neglected with $t_{22} = 0$ as an approximation, which is consistent to the approximation considered in even-even nuclei within vibration to γ-soft transitional region in the interacting boson model [37]. Hence, $T^{(2)}_F$ is responsible for $\Delta\tau = 0$ transitions, while the core part $T^{(2)}_C$ is responsible for $\Delta\tau = +1$ and -1 transitions. In the following, we set $\xi = (t'_{22}/t_{21})$.

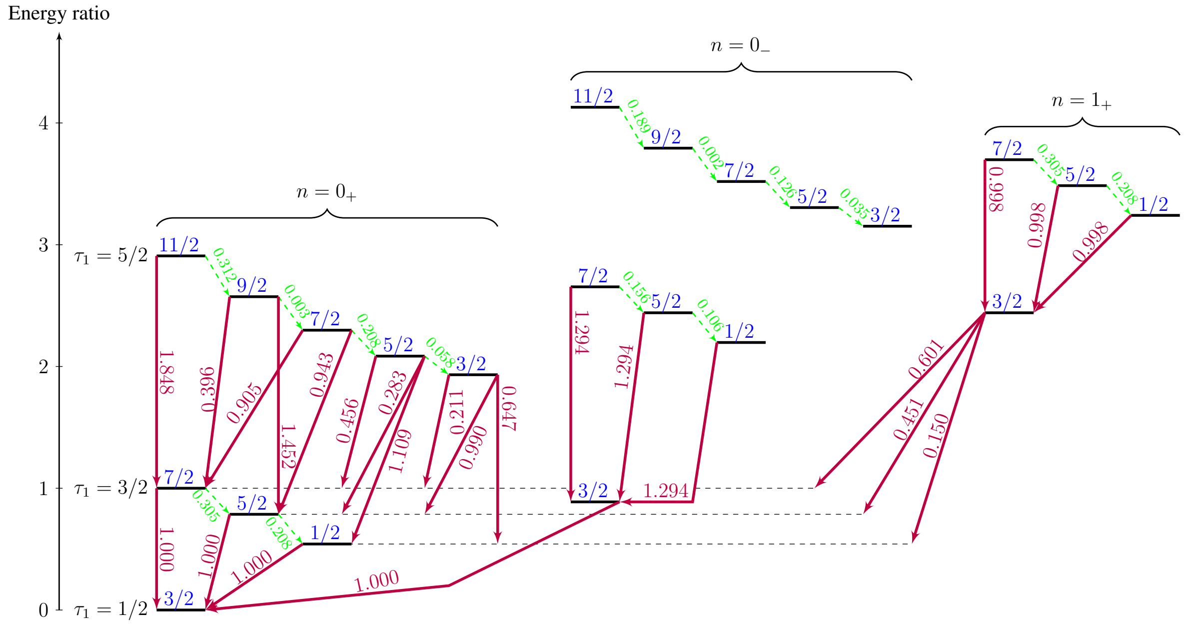

Figure 1: Energy ratios and B(E2) values of the model, where the parameters are set with $a = 2, b = 4, k = -0.5, k' = 0.3$ and $\xi = 0.25$. The solid lines are the level energies normalized to the first $7/2$ level energy, red solid line with arrows represent B(E2) values normalized to B(E2; $7/2_1 \to 3/2_1$), which satisfy the selection rule $\Delta\tau = \pm 1$, while the green dashed line with arrows represent B(E2) values normalized to B(E2; $7/2_1 \to 3/2_1$) with the selection rule $\Delta\tau = 0$. The left part of the levels are those with $n = 0_+$, the middle part of the levels are those with $n = 0_-$, and the right part of the levels are those with $n = 1_+$, for which the sign in the subscript is the sign in $\tau_1 = \tau \pm \frac{1}{2}$.

Fig. 1 provides typical level and E2 transition patterns of the model, for which the parameters are set as $a = 2, b = 4, k = -0.5, k' = 0.3$, and $\xi = 0.25$. There are three parts in Fig. 1. The first part from the left contains the levels with $n = 0_+$, the middle part contains those with $n = 0_-$, where the $\pm$ sign indicates $\tau_1 = \tau \pm 1/2$. The excited energy levels are shown by black solid lines. All transitions are normalized to B(E2; $0, 1, 3/2, 7/2 \to 0, 1, 1/2, 3/2$) and shown by the colored arrows. B(E2) values shown by the red solid lines and green dashed lines with arrow are for $\Delta\tau = \pm 1$ and $\Delta\tau = 0$ transitions, respectively.

To test the validity of the model, we use it to reproduce experimental available data of ^{187,189,191,193,195}Ir [38–42]. Table 2 shows the results of the fit for the energy ratios, which consists of three parts. The top part contains the theoretical predictions with $n = 0_+$ and the corresponding experimental data. The middle part contains those with $n = 0_-$. The bottom part provides the parameters of the model used for each nucleus and the corresponding χ^2 value. The first three columns of the two tables are quantum numbers of the corresponding state in the model. The dashed lines represent that there is no experimental value available. Except for those experimentally undetermined level energies, the χ^2 value for the known level energies of the 5 odd-A nuclei fitted shows that they are well reproduced by this model, especially for ^{195}Ir. The average value of χ^2 for level energy ratios of all the nuclei fitted is $\overline{\chi^2} = 0.053$.

Table 2: Energy ratios of ^{187,189,191,193,195}Ir fitted by the model, where the experimental data are taken from [38–42].

States					^{187}Ir		^{189}Ir		^{191}Ir		^{193}Ir		^{195}Ir	
M	n	τ	τ_1	J	Theo.	Exp.	Theo.	Exp.	Theo.	Exp.	Theo.	Exp.	Theo.	Exp.
1	0	0	1/2	3/2	0.000	0.000	0.000	0.000	0.000	0.000	0.000	0.000	0.000	0.000
1	0	1	3/2	1/2	0.242	0.373	0.373	0.314	0.297	0.240	0.257	0.204	0.202	0.176
1	0	1	3/2	5/2	0.646	0.386	0.708	0.379	0.672	0.377	0.653	0.388	0.627	0.445
1	0	1	3/2	7/2	1.000	1.000	1.000	1.000	1.000	1.000	1.000	1.000	1.000	1.000
0	0	2	5/2	3/2	0.835	0.665	1.012	0.588	0.875	0.521	0.812	0.503	0.772	0.727
0	0	2	5/2	5/2	1.087	1.093	1.221	1.057	1.109	1.023	1.060	1.011	1.038	1.046
0	0	2	5/2	7/2	1.441	1.653	1.513	1.547	1.437	1.469	1.406	1.443	1.410	—
0	0	2	5/2	9/2	1.895	1.554	1.889	1.511	1.859	1.464	1.852	1.459	1.889	—
0	0	2	5/2	11/2	2.451	2.515	2.349	2.482	2.375	2.424	2.396	2.396	2.475	—
0	0	3	7/2	5/2	1.491	—	1.722	2.144	1.546	1.713	1.466	1.563	1.410	1.477
0	0	3	7/2	7/2	1.845	—	2.015	2.506	1.875	1.999	1.812	1.736	1.782	—
0	0	3	7/2	9/2	2.299	—	2.391	2.393	2.297	2.365	2.258	2.345	2.261	—
0	0	3	7/2	9/2	2.299	2.415	2.391	2.393	2.297	2.404	2.258	2.494	2.261	—
0	0	3	7/2	11/2	2.855	3.148	2.851	2.993	2.813	2.888	2.802	2.821	2.847	—
0	0	3	7/2	13/2	3.512	3.168	3.394	3.056	3.422	2.924	3.446	2.895	3.539	—
0	0	3	7/2	15/2	4.270	4.435	4.020	4.314	4.126	4.132	4.188	4.081	4.337	—
1	0	1	1/2	3/2	3.070	—	1.773	2.144	1.222	1.713	1.118	1.288	0.632	0.593
0	0	2	3/2	1/2	4.429	4.405	2.671	2.506	1.833	1.818	1.660	1.558	0.991	1.088
0	0	2	3/2	5/2	4.833	—	3.005	2.829	2.208	2.179	2.056	1.943	1.417	1.268
0	0	2	3/2	7/2	5.187	—	3.298	—	2.536	2.404	2.403	—	1.789	—
0	0	3	5/2	3/2	6.055	—	3.808	—	2.725	—	2.499	—	1.631	—
0	0	3	5/2	5/2	6.308	—	4.017	—	2.959	—	2.747	—	1.897	1.930
0	0	3	5/2	7/2	6.661	—	4.309	—	3.287	—	3.093	—	2.269	—
0	0	3	5/2	9/2	7.116	—	4.685	—	3.709	3.515	3.539	—	2.748	—
0	0	3	5/2	11/2	7.672	—	5.145	—	4.225	—	4.083	—	3.334	—
a					0.50		2.20		0.01		0.01		3.68	
b					9.39		32.06		26.10		21.38		16.53	
k					−10.70		−21.60		−13.79		−11.10		−4.20	
k'					1.01		3.54		4.12		3.86		4.13	
χ^2					0.052		0.094		0.058		0.052		0.011	

Table 3: B(E2) values for the transitions in ^{187,189,191,193,195}Ir obtained from the model with $g(\beta) = \frac{\hbar^2}{2B}$ and the parameters shown in Table 2.

M	n	τ	τ_1	J	M'	n'	τ'	τ_1'	J'	$\|\Delta\tau\|$	^{187}Ir	^{189}Ir	^{191}Ir	^{193}Ir	^{195}Ir
1	0	1	3/2	7/2	1	0	0	1/2	3/2	1	1.000	1.000	1.000	1.000	1.000
1	0	1	3/2	5/2	1	0	0	1/2	3/2	1	1.000	1.000	1.000	1.000	1.000
1	0	1	3/2	1/2	1	0	0	1/2	3/2	1	1.000	1.000	1.000	1.000	1.000
0	0	2	5/2	11/2	1	0	1	3/2	7/2	1	1.989	1.996	2.000	2.000	1.974
0	0	2	5/2	9/2	1	0	1	3/2	7/2	1	0.426	0.428	0.429	0.429	0.423
0	0	2	5/2	9/2	1	0	1	3/2	5/2	1	1.563	1.568	1.571	1.571	1.551
0	0	2	5/2	7/2	1	0	1	3/2	7/2	1	0.974	0.978	0.980	0.980	0.967
0	0	2	5/2	7/2	1	0	1	3/2	5/2	1	1.015	1.018	1.020	1.020	1.007
0	0	2	5/2	5/2	1	0	1	3/2	7/2	1	0.491	0.493	0.494	0.494	0.487
0	0	2	5/2	5/2	1	0	1	3/2	5/2	1	0.304	0.305	0.306	0.306	0.302
0	0	2	5/2	5/2	1	0	1	3/2	1/2	1	1.193	1.197	1.200	1.200	1.184
0	0	2	5/2	3/2	1	0	1	3/2	7/2	1	0.227	0.228	0.229	0.229	0.226
0	0	2	5/2	3/2	1	0	1	3/2	5/2	1	1.065	1.069	1.071	1.071	1.057
0	0	2	5/2	3/2	1	0	1	3/2	1/2	1	0.696	0.699	0.700	0.700	0.691
0	0	3	7/2	15/2	0	0	2	5/2	11/2	1	2.937	2.975	3.000	3.000	2.865
0	0	3	7/2	13/2	0	0	2	5/2	11/2	1	0.267	0.270	0.273	0.273	0.260
0	0	3	7/2	13/2	0	0	2	5/2	9/2	1	2.670	2.705	2.727	2.727	2.605
0	0	3	7/2	11/2	0	0	2	5/2	11/2	1	1.013	1.026	1.034	1.034	0.988
0	0	3	7/2	11/2	0	0	2	5/2	9/2	1	0.385	0.390	0.393	0.393	0.375
0	0	3	7/2	11/2	0	0	2	5/2	7/2	1	1.540	1.560	1.573	1.573	1.502
0	0	2	3/2	7/2	1	0	1	1/2	3/2	1	1.392	1.397	1.400	1.400	1.382
0	0	2	3/2	5/2	1	0	1	1/2	3/2	1	1.392	1.397	1.400	1.400	1.382
0	0	2	3/2	1/2	1	0	1	1/2	3/2	1	1.392	1.397	1.400	1.400	1.382
1	0	1	1/2	3/2	1	0	0	1/2	3/2	1	1.000	1.000	1.000	1.000	1.000
1	1	1	3/2	7/2	1	1	0	1/2	3/2	1	1.349	1.380	1.400	1.400	1.293
1	1	1	3/2	5/2	1	1	0	1/2	3/2	1	1.349	1.380	1.400	1.400	1.293
1	1	1	3/2	1/2	1	1	0	1/2	3/2	1	1.349	1.380	1.400	1.400	1.293
1	1	0	1/2	3/2	1	0	1	3/2	7/2	1	0.784	0.794	0.800	0.800	0.764
1	1	0	1/2	3/2	1	0	1	3/2	5/2	1	0.588	0.596	0.600	0.600	0.573
1	1	0	1/2	3/2	1	0	1	3/2	1/2	1	0.196	0.199	0.200	0.200	0.191
1	0	1	3/2	7/2	1	0	1	3/2	5/2	0	9.741 ξ^2	33.082 ξ^2	0.604	21.992 ξ^2	17.353 ξ^2
1	0	1	3/2	5/2	1	0	1	3/2	1/2	0	6.630 ξ^2	22.514 ξ^2	0.411	14.966 ξ^2	11.810 ξ^2
0	0	2	5/2	11/2	0	0	2	5/2	9/2	0	9.949 ξ^2	33.788 ξ^2	0.617	22.461 ξ^2	17.723 ξ^2
0	0	2	5/2	9/2	0	0	2	5/2	7/2	0	0.103 ξ^2	0.350 ξ^2	0.006	0.233 ξ^2	0.184 ξ^2
0	0	2	5/2	7/2	0	0	2	5/2	5/2	0	6.645 ξ^2	22.568 ξ^2	0.412	15.002 ξ^2	11.838 ξ^2
0	0	2	5/2	5/2	0	0	2	5/2	3/2	0	1.855 ξ^2	6.301 ξ^2	0.115	4.189 ξ^2	3.305 ξ^2
0	0	2	3/2	7/2	0	0	2	3/2	5/2	0	4.970 ξ^2	16.879 ξ^2	0.308	11.220 ξ^2	8.854 ξ^2
0	0	2	3/2	5/2	0	0	2	3/2	1/2	0	3.382 ξ^2	11.487 ξ^2	0.210	7.636 ξ^2	6.025 ξ^2
0	0	3	5/2	11/2	0	0	3	5/2	9/2	0	6.019 ξ^2	20.440 ξ^2	0.373	13.587 ξ^2	10.721 ξ^2
0	0	3	5/2	9/2	0	0	3	5/2	7/2	0	0.062 ξ^2	0.212 ξ^2	0.004	0.141 ξ^2	0.111 ξ^2
0	0	3	5/2	7/2	0	0	3	5/2	5/2	0	4.020 ξ^2	13.652 ξ^2	0.249	9.075 ξ^2	7.161 ξ^2
0	0	3	5/2	5/2	0	0	3	5/2	3/2	0	1.122 ξ^2	3.812 ξ^2	0.070	2.534 ξ^2	2.000 ξ^2
1	1	1	3/2	7/2	1	1	1	3/2	5/2	0	9.741 ξ^2	33.082 ξ^2	0.604	21.992 ξ^2	17.353 ξ^2
1	1	1	3/2	5/2	1	1	1	3/2	1/2	0	6.630 ξ^2	22.514 ξ^2	0.411	14.966 ξ^2	11.810 ξ^2

Table 4: A comparison of the theoretical results with the corresponding experimental B(E2) values for ^{191,193}Ir, where "—" denotes the corresponding value not observed experimentally.

Initial state	Final state	^{191}Ir		^{193}Ir	
$(M,\ n,\ \tau,\ \tau_1,\ \ J)$	$(M',\ n',\ \tau',\ {\tau_1}',\ \ J')$	Exp.	Theo.	Exp.	Theo.
$(1,\ 0,\ 1, 3/2, 7/2)$	$(1,\ 0,\ 0,\ 1/2, 3/2)$	1.000	1.000	1.000	1.000
$(1,\ 0,\ 1, 3/2, 5/2)$	$(1,\ 0,\ 0,\ 1/2, 3/2)$	2.296	1.000	2.601	1.000
$(1,\ 0,\ 1, 3/2, 1/2)$	$(1,\ 0,\ 0,\ 1/2, 3/2)$	0.499	1.000	0.700	1.000
$(0,\ 0,\ 2, 5/2, 11/2)$	$(1,\ 0,\ 1,\ 3/2, 7/2)$	—	2.000	1.765	2.000
$(0,\ 0,\ 2, 5/2, 9/2)$	$(1,\ 0,\ 1,\ 3/2, 5/2)$	1.718	1.571	—	1.571
$(0,\ 0,\ 2, 5/2, 3/2)$	$(1,\ 0,\ 1,\ 3/2, 5/2)$	0.644	1.071	1.889	1.071
$(0,\ 0,\ 2, 5/2, 3/2)$	$(1,\ 0,\ 1,\ 3/2, 1/2)$	1.384	0.700	1.703	0.700
$(1,\ 0,\ 1, 3/2, 5/2)$	$(1,\ 0,\ 1,\ 3/2, 1/2)$	0.248	0.411	—	14.966 ξ^2
$(1,\ 0,\ 1, 3/2, 7/2)$	$(1,\ 0,\ 1,\ 3/2, 5/2)$	0.711	0.604	—	21.992 ξ^2

Once the model parameters are determined from the fitting to the level energies, some B(E2) values of the transitions among the states of the ground band and first excited band are also calculated, in which, except for ^{191}Ir, the ratio ξ for the other 4 nuclei can not be determined due to there is in lack of experimental data of $\Delta\tau = 0$ transitions. Due to only a few experimental data of B(E2) values are known, a reliable analysis of the model is still not all possible. With the only two known $\Delta\tau = 0$ B(E2) values in ^{191}Ir, $\xi = 0.15$ is taken for ^{191}Ir. A comprehensive predictions of normalized B(E2) values are listed in Table 3. It is seen that only for ^{191}Ir we are able to fully predict $\Delta\tau = 0$ transitions.

Table 4 provides the model results of some B(E2) values and the corresponding experimentally measured B(E2) values for ^{191,193}Ir. In concerning the fitting results of the level energies and the experimentally available B(E2) values, it is shown that the model with the β-independent five-dimensional spin-orbit interaction $\hat{\Lambda} \circ \hat{\Sigma}$ and the total angular momentum degeneracy breaking term seems suitable to describe the γ-unstable odd-A Ir isotopes, though further analysis of other odd-A nuclei in this region are necessary.

5 Summary

In this paper, odd-A nuclei are studied within the collective model of the γ-unstable Bohr Hamiltonian with the quasi exactly solvable sextic potential known previously. A β-independent five-dimensional spin-orbit interaction and the total angular momentum degeneracy breaking term are considered in the model Hamiltonian. Analytical form of energy eigenvalues and eigenfunctions are derived. Typical level and E2 transition patterns of the model are demonstrated. To test the validity of this coupling scheme, we use the model to reproduce experimental available data of ^{187,189,191,193,195}Ir. It is clearly shown from the level energies fitted that the model with the β-independent five-dimensional spin-orbit interaction and the total angular momentum degeneracy breaking term reproduces the experimental data very well with the average value of χ^2 for level energie ratios of these 5 nuclei to be $\overline{\chi^2} = 0.053$. Some B(E2) values of the model are also evaluated. Though there are only a few experimental B(E2) values for ^{191,193}Ir are available, we find a good agreement between the theoretical predictions and avaiable experimental data. Thus, the model with the β-independent five-dimensional spin-orbit interaction $\hat{\Lambda} \circ \hat{\Sigma}$ and the total angular momentum degeneracy breaking term seems suitable to describe these odd-A nuclei. However, further analysis is necessary to see whether the model with the β-independent five-dimensional spin-orbit interaction and the total angular momentum degeneracy breaking term is also suitable to describe other odd-A nuclei in the same mass region. Numerical solution of the sextic potential without the quasi-exactly solvable constraints should provide more accurate results of the model, which will be a part of our future work.

Acknowledgement: The authors are grateful to the referee for helpful comments and suggestions on this work. Support from the National Natural Science Foundation of China (11675071), the Liaoning Provincial Universities Overseas Training Program (2019-46), the U. S. National Science Foundation (OIA-1738287 and ACI-1713690), U. S. Department of Energy (DE-SC0005248), the Southeastern Universities Research Association, and the LSU-LNNU joint research program (9961) is acknowledged.

References

[1] F. Iachello, *Phys. Rev. Lett.* **85** 3580 (2000).

[2] F. Iachello, *Phys. Rev. Lett.* **87** 052502 (2001).

[3] F. Iachello, A. Arima, The Interacting Boson Model, Cambridge University Press, Cambridge, England, 1987.

[4] J. H. Ginocchio, M. W. Kirson, Phys. Rev. Lett. 44 (1980) 1744;

[5] A. E. L. Dieperink, O. Scholten, F. Iachello, Phys. Rev. Lett. 44 (1980) 1747.

[6] P. Cejnar, J. Jolie and R. F. Casten, *Rev. Mod. Phys.* **82** 2155 (2010).

[7] R. F. Casten and E. A. McCutchan, *J. Phys. G: Nucl. Part. Phys.* **34** R285 (2007).

[8] L. Fortunato, *Eur. Phys. J. A* **26** 1 (2005).

[9] P. Buganu, L. Fortunato, *J. Phys. G: Nucl. Part. Phys.* **43** 093003 (2016).

[10] A. Bohr, *Mat. Fys. Medd. K. Dan. Vidensk. Selsk.* **26** 14 (1952).

[11] A. Bohr, B. R. Mottelson, *Mat. Fys. Medd. K. Dan. Vidensk, Selsk.* **27** 16 (1953).

[12] D. Bonatsos, D. Lenis, N. Minkov, D. Petrellis, P. P. Raychev and P. A. Terziev, *Phys. Rev. C* **70** 024305 (2004).

[13] D. Bonatsos, D. Lenis, N. Minkov, D. Petrellis, P.P. Raychev, P.A. Terziev, *Phys. Lett. B* **584** 40 (2004)

[14] F. Iachello, *Phys. Rev. Lett.* **95** 052503 (2005).

[15] M. A. Caprio and F. Iachello, *Nucl. Phys. A* **781** 26 (2007).

[16] C. E. Alonso, J. M. Arias, and A. Vitturi, *Phys. Rev. Lett.* **98** 052501 (2007).

[17] C. E. Alonso, J. M. Arias, and A. Vitturi, *Phys. Rev. C* **75** 064316 (2007).

[18] Yu Zhang, Feng Pan, Yu-Xin Liu, Zhan-Feng Hou, and J. P. Draayer, *Phys. Rev. C* **82** 034327 (2010).

[19] Yu Zhang, Feng Pan, Yu-Xin Liu, Yan-An Luo, and J. P. Draayer, *Phys. Rev. C* **84** 034306 (2011).

[20] H. Hassanabadi and H. Sobhani, *Nucl. Phys. A* **986** 223 (2019).

[21] H. Sobhani and H. Hassanabadi, *Nucl. Phys. A* **992** 121621 (2019).

[22] I. Inci and H. Sonkaya *Int. J. Mod. Phys. E* **27** (10) 1850085 (2018).

[23] A. G. Ushveridze, *Quasi-exactly solvable models in quantum mechanics*, IOP, Bristol, (1994).

[24] G. Lévai and J. M. Arias, *Phys. Rev. C* **69** 014304 (2004).

[25] G. Lévai and J. M. Arias, *Phys. Rev. C* **81** 044304 (2010).

[26] A. A. Raduta, P. Buganu, *Phys. Rev. C* **83** 034313 (2011).

[27] A. A. Raduta, P. Buganu, *J. Phys. G: Nucl. Part. Phys.* **40** 025108 (2013).

[28] P. Buganu. R. Budaca, *Phys. Rev. C* **91** 014306 (2015).

[29] P. Buganu, R. Budaca, *J. Phys. G: Nucl. Part. Phys.* **42** 105106 (2015).

[30] R. Budaca, P. Buganu, M. Chabab, A. Lahbas, M. Oulne, *Ann. Phys. (NY)* **375** 65 (2016).

[31] A. Lahbas, P. Buganu, R. Budaca, *Mod. Phys. Lett. A* **35** 2050085 (2020).

[32] D. R. Bés, Nucl. Phys. 10 (1959) 373.

[33] Hadi Sobhani, Hassan Hassanabadi, Dennis Bonatsos, Feng Pan, Sai Cui, Ziwei Feng, Jerry P Draayer, *Eur. Phys. J. A* **56** 29 (2020).

[34] D. J. Rowe, P. S. Turner, J. Repka, *J. Math. Phys.* **45** 2761 (2004).

[35] R. Budaca, *Eur. Phys. J. A* **52** 314 (2016).

[36] F. Pan, L. Bao, Y.-Z. Zhang, J. P. Draayer, *Eur. Phys. J. Plus* **129** 169 (2014).

[37] F. Iachello, P. Van Isacker, The Interacting Boson-Fermion Model, Cambridge Univ. Press, Cambridge, 1991.

[38] M. S. Basunia, *Nucl. Data Sheets* **110** 999 (2009).

[39] T. D. Johnson and B. Singh, *Nucl. Data Sheets* **142** 1 (2017).

[40] V. R. Vanin, N. L. Maidana, R. M. Castro, E. Achterberg, O. A. Capurro, and G. V. Martí *Nucl. Data Sheets* **108** 2393 (2007).

[41] A. Artna-Cohen, *Nucl. Data Sheets* **83** 921 (1998).

[42] X. Huang and M. Kang, *Nucl. Data Sheets* **121** 395 (2014).